Anat Embryol (1989) 180:17–28

Anatomy
and Embryology

Original articles

The developing neuroepithelium in human embryonic and fetal brain studied with vimentin-immunocytochemistry

Mette Stagaard and Kjeld Møllgård

Department of Medical Anatomy A and the Neuroscience Center, The Panum Institute, Blegdamsvej 3, DK-2200 Copenhagen N, Denmark

Summary. The neuroepithelial cells, which constitute the primordium of the CNS, are potentially capable of generating neuronal and glial cell lineages concomitantly. The appearance and morphological development of vimentin-positive neuroepithelial cells in human embryonic and fetal brain (4–16 weeks) were studied with immunocytochemistry. In embryos aged 4–6 weeks, vimentin-reactivity was seen in all neuroepithelial cells, including those which exhibited mitotic figures. The distribution of reactivity changed according to a general developmental pattern, which commenced and proceeded temporally different in various regions of the CNS. All regions exhibited vimentin-positive neuroepithelial cells, the distribution and morphology of which gradually changed, resulting in lamination of the neural wall into two and subsequently three layers. The neocortex and midline raphe were the only regions to differ significantly from the general pattern. When reactivity to glial fibrillary acidic protein developed at 7–8 weeks, the distribution was very much like that of vimentin at the same stage. Reactivity to glial, neuronal and other cellular markers (S-100, neurofilament, neuron specific enolase, desmin, and cytokeratin) revealed different distributions. Although cells retaining vimentin beyond the ventricular zone stage are radial glial cells and presumptive fibrous astrocytes, it seems unlikely that vimentin is a marker for a distinct cell lineage during early CNS development. It is suggested that all neuroepithelial cells in vivo differentiate to a stage where they express vimentin, and that vimentin may have a functional role in cellular movements and during the interkinetic nuclear migration.

Key words: Human brain development – Neuroepithelium – Vimentin – Intermediate filaments

Introduction

Several lines of investigation have focused on the first appearance and subsequent differentiation of neurons in early vertebrate brain development. Golgi, electronmicroscopic, and autoradiographic studies have thus successfully identified and birthdated various neuronal populations (e.g. Rakic 1971; Choi and Lapham 1978; for review see Varon and Somjen 1979). The question of glial cell development has, though, been a matter of continued controversy since the original proposal of His (1889), that two separate precursors coexist in the germinal zones. In more recent years, the concept of His has been further substantiated by the demonstration of glial fibrillary acidic protein (GFA) immunoreactivity in a subpopulation of ventricular cells in the lateral telencephalic wall of monkey fetuses (Levitt and Rakic 1980; Levitt et al. 1983). At a comparable developmental stage at the appearance of the cortical plate, GFA

Offprint requests to: M. Stagaard

Table 1

Number	CRL, mm	Fixative
Embryos		
1	4.5	10% buffered formalin
2	5.5	10% buffered formalin
3	7	Bouin's fixative
4	9	10% buffered formalin
5	15	2.5% glutaraldehyde
6	16	Lillie's fixative
7	20	10% buffered formalin
8	21	10% buffered formalin
9	21.5	10% buffered formalin
10	23	10% buffered formalin
11	23	Formol-Calcium
12	24	Formol-Calcium
13	26	Lillie's fixative
14	28	Lillie's fixative
15	31	Formol-Calcium
16	31.5	Lillie's fixative
17	32	Lillie's fixative
18	38	Lillie's fixative
19	38	10% buffered formalin
Fetuses		
20	42	Formol-Calcium
21	44	Formol-Calcium
22	45	10% buffered formalin
23	52	Lillie's fixative
24	54	Formol-Calcium
25	59	Formol-Calcium
26	62	Formol-Calcium
27	62	10% buffered formalin
28	81	10% buffered formalin
29	92	Formol-Calcium
30	101	10% buffered formalin
31	144	Formol-Calcium
32	148	Formol-Calcium
33	149	Formol-Calcium
34	168	Formol-Calcium
35	168	Formol-Calcium
36	168	Bouin's fixative

Table 2. Antibodies

Anti-	Company	Code	Antigen source	Antibody source	Clone	Dilution
Vimentin	Dakopatts, DK	M 725	Swine	Mouse	V9[a]	1:500
	Sigma, USA	V 4630	Human	Goat		1:100
	Sigma, USA	V 5255	Human	Mouse	VIM 13.2	1:10
	Labsystems, SF	6400 301	Human	Mouse	–	1:10
GFA	Dakopatts, DK	Z 334	Cow	Rabbit[b]		1:250
	Dakopatts, DK	M 761	Human	Mouse	GF-2	1:25
	Medac, FRD	GFP	Human	Rabbit[b]		1:1000
	Labsystems, SF	6400 101	Human	Mouse	–	1:200
	Amersham, UK	RPN 1106	Human	Mouse	–	1:5
NF						
70 & 200 kD	Dakopatts, DK	M 762	Human	Mouse	2F11	1:25
200 kD	Labsystems, SF	6400 501	Cow	Mouse	–	1:500
160 kD	Amersham, UK	RPN 1104	Swine	Mouse	–	1:10
Cytokeratin						
8	Amersham, UK	RPN 1166	Human	Mouse	–	1:5
18	Sanbio, NL	F 3006	Human	Mouse	M9	1:10
56 & 64 kD	Dakopatts, DK	A 575	Human	Rabbit		1:400
6 & 18	Dakopatts, DK	M 717	Human	Mouse	LP 34	1:100
8, 18 & 19	Becton-Dickinson	7650	Human	Mouse	CAM 5.2	1:1
Desmin	Dakopatts, DK	A 611	Chicken	Rabbit		1:500
NSE	Dakopatts, DK	A 589	Cow	Rabbit		1:2000
S-100	Dakopatts, DK	Z 311	Cow	Rabbit		1:1000

[a] Osborn et al. 1984
[b] Anti-GFA antibodies were preadsorbed with NF antigens (cf. Hansen et al. 1989)

has been detected in radial glial cells in human fetal frontoparietal cortex (Antanitus et al. 1976; Choi and Lapham 1978), and somewhat earlier in human fetal spinal cord (Choi 1981; Lauriola et al. 1987).

In various experimental animals, the intermediate filament vimentin has been detected at very early stages of CNS development (rat: Dahl et al. 1981; Bignami et al. 1982; mouse: Schnitzer et al. 1981; Houle and Fedoroff 1983; Cochard and Paulin, 1984; rabbit: Viebahn et al. 1988; chicken: Tapscott et al. 1981; Bennett and DiLullo 1985; quail: Erickson et al. 1987; canary: Alvarez-Buylla et al. 1987; and *Xenopus laevis*: Szaro and Gainer 1988). Vimentin has been described as being transiently expressed in neuroepithelial cells, and to appear at a stage when 15–20 somites have developed (Houle and Fedoroff 1983). It has been suggested that the vimentin-reactivity either overlapped with or was replaced by GFA-reactivity (e.g. Dahl 1981; Dahl et al. 1981; Bovolenta et al. 1984).

In the present study we have investigated the temperospatiel distribution and morphology of the vimentin-positive neuroepithelial cells in human embryos and fetuses. In order to further characterize the vimentin-positive cell population, a comparison was made with the immunoreactivity patterns of other cellular markers: GFA, S-100, neurofilament protein (NF) and neuron specific enolase (NSE), as well as with desmin and cytokeratin.

Material and methods

A total of 19 embryos and 17 fetuses were examined. The embryos and fetuses, which ranged from 4.5–168 mm crown-rump length (CRL) corresponding to 4–16 weeks of gestation, were obtained from Caesarean sections in connection with legal abortions or from extrauterine pregnancies. Immediately following the operation the entire embryo or the fetal brain, dissected into appropriate blocks, were fixed for 12–24 h at 4° C in one of the following fixatives: 10% buffered formalin, 2.5% buffered glutaraldehyde, 4% Formol-Calcium, Lillie's or Bouin's fixatives (Table 1). Specimens were dehydrated in graded alcohols, cleared in xylene and embedded in paraffin wax at 58° C. Serial 3–5 μm sections were cut in frontal, sagittal or horizontal planes. Tissue blocks of three fetuses, fixed for 12 h in 4% buffered paraformaldehyde, were either embedded in low-melting point (52° C) paraffin wax, or cryoprotected in 30% sucrose prior to embedding in Tissue-Tek and the cutting of 8–10 μm sections at −18 to −22° C.

Immunocytochemical procedure. Paraffin-embedded sections were rehydrated and washed in 0.05 M Tris, 0.15 M NaCl and 0.01% Nonidet P-40, pH 7.4 (TBS-Nonidet), and then incubated in the diluting buffer solution: 10% normal goat serum in TBS. Overnight incubation with the primary antibody (see Table 2) was carried out at 4° C. Sections were washed 15 min in 3 changes of TBS-Nonidet before 30 min incubation with the secondary antibody: rabbit-anti-mouse IgG (1:20, Dakopatts, DK) or biotinylated swine-anti-rabbit IgC (1:300, Dakopatts, DK). The sections were washed and incubated for 30 min in either mouse PAP (1:50, Dakopatts, DK) or streptavidin-horseradish peroxidase (1:300, Amersham, UK). After further washing the reaction was developed stepwise in 0.03% diaminoben-

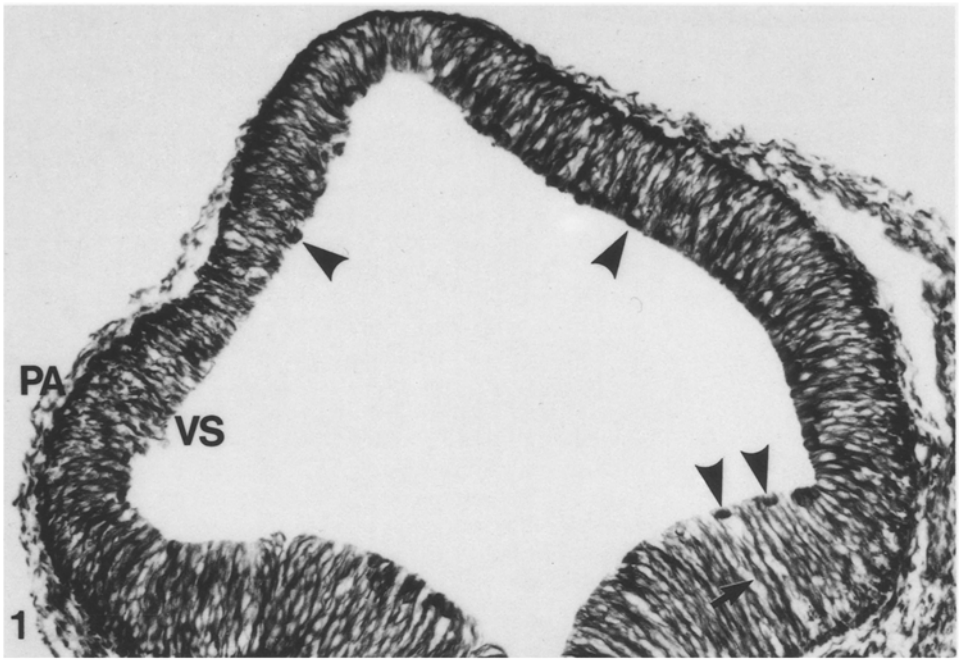

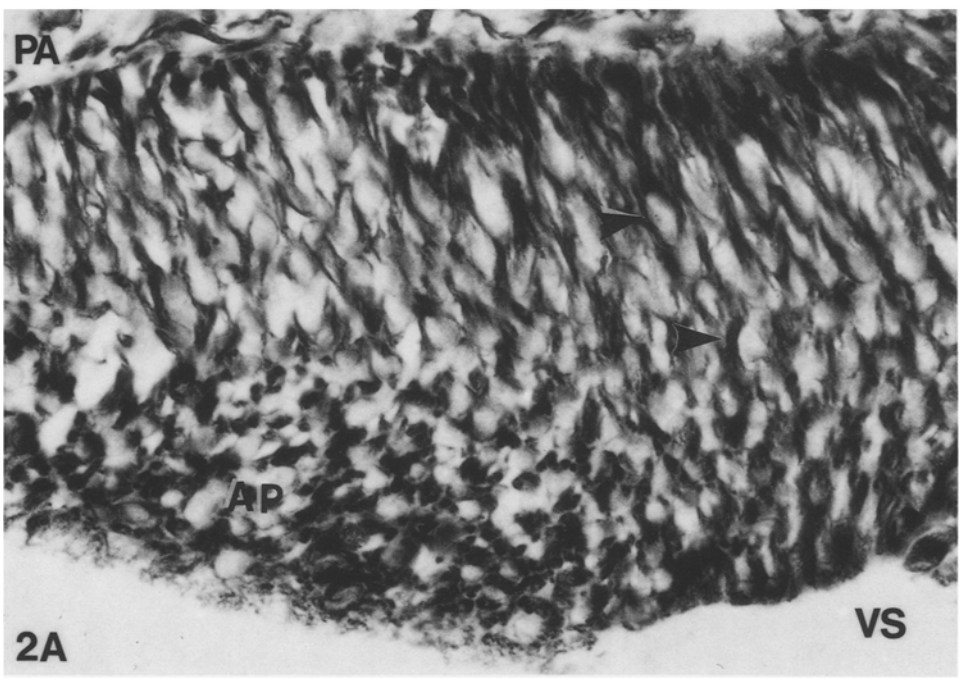

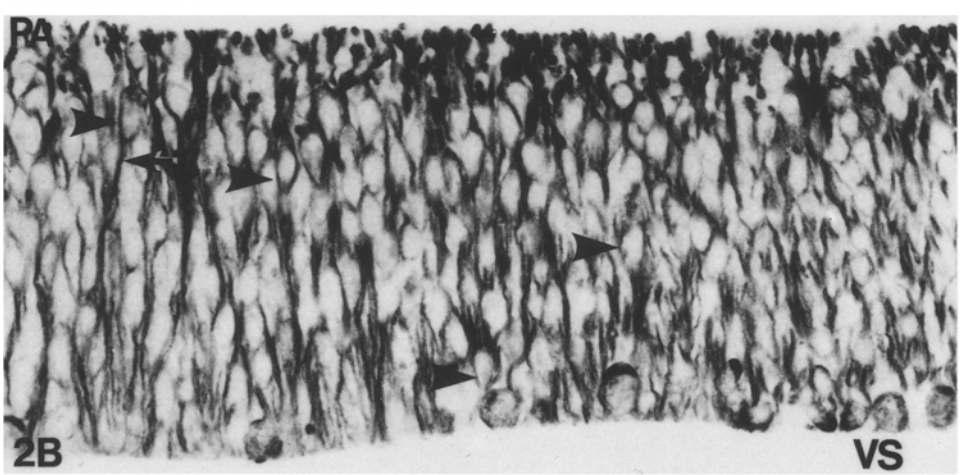

Fig. 1. All NE cells in the prosencephalon of a 7 mm CRL embryo are vimentin-positive, and span the neural wall (*arrow*) from the ventricular surface (*VS*) to the external, presumptive pia-arachnoid surface (*PA*). *Arrowheads* indicate mitoses. ×215

Fig. 2. **A** Neural tube, 4.5 mm CRL. **B** Rhombencephalon, 7 mm CRL. The endfeet facing the presumptive pia-arachnoid (*PA*) are closely packed. Perinuclear vimentin-reactivity is seen throughout the pseudostratified neuroepithelium (*arrowheads*), and apical vimentin-positive processes (*arrow* in **B**) extend to the ventricular surface (*VS*). In (**A**) apical processes (*AP*) are cross-sectioned in a tangential cut. **A** ×800 **B** ×575

zidine (DAB) in TBS for 10 min, and then in 0.015% H_2O_2 DAB-TBS pH 7.4 for 10 min. The sections were dehydrated and coverslipped with DPX.

The specimens treated with fixatives containing paraformaldehyde, exhibiting acceptable to good morphology, revealed only minor differences in the immunoreactivity to the various antibodies used. Embedding in 52° C paraffin wax did not significantly enhance immunoreactivity, likewise, the cryo-sectioning did not convincingly improve reactivity to the antibodies used in the present study. Thus, the state of the tissue prior to fixation was found to be the factor, that determined the final result. Selected sections were treated with 0.1% pancreatic trypsin, type II (Sigma) in 0.05 M Tris, 0.1% $CaCl_2$, pH 7.8 for 5–20 min at 37° C. Trypsin treatment enhanced the reactivities to anti-GFA and anti-cytokeratin antibodies and to the monoclonal anti-vimentin antibody from Labsystems.

Terminology. The specific terms previously used in the description of human neocortical development (Marin-Padilla 1983; Møllgård and Jacobsen 1984) is related to the appearance of a cortical plate. As the characteristics of the development of the neocortex are not distinctly reflected in the pattern of vimentin-reactivity, these terms are not applied; thus, only the general terms for describing the different stages of CNS development proposed by the Boulder Committee (1970) are used throughout this study.

Results

General pattern of vimentin-reactivity

In the youngest embryos (4.5–9 mm CRL) which represent the ventricular zone stage, the vimentin-immunoreactivity was impressive: all cells throughout the pseudostratified neuroepithelium of the neural tube were positive (Figs. 1; 2A, B). In sections cut perpendicular to the ventricular system, the vimentin-positive neuroepithelial (NE) cells could be followed as thick radial processes from the ventricular surface to the external surface, where the pia-arachnoid shall later develop (Fig. 1). The deeper-lying NE cells were outlined by perinuclear immunostaining, and they had processes from the apical and basal poles to the ventricular and external surfaces, respectively (Fig. 2A, B). Being displaced by other NE cell nuclei, the thick radial processes followed a tortuous path towards the external limiting membrane, where they terminated in prominent bulbous endfeet. At this stage the endfeet were closely packed (Fig. 2A, B), and thus formed a continuous layer facing the basement membrane and the presumptive pia-arachnoid.

With the development of a marginal zone (MZ) the pattern of vimentin-immunoreactive processes was altered, so that the ventricular zone (VZ) continued to exhibit the thick radial processes, whereas the processes in the newly developed MZ were thin, straight and few in number. The majority of these processes was also radially orientated, but some ran perpendicular to the radial ones (Fig. 3). The difference of process density and direction gave the neuroepithelium a bilayered appearance. This change first occurred at 9 mm CRL in the lower rhombencephalon. From this level the development of MZ and the subsequent lamination extended rostrally and caudally to include the entire CNS, reaching the telencephalon at about 7 weeks (15 mm CRL). At this stage of development a new, third layer was developing in the lower rhombencephalon. This middle layer was composed of thin radial processes, which were in continuity with the thick processes in VZ, as well as with those in the MZ. The point at which the finer and scarcer processes could be distinguished coincided with the development of an intermediate zone (IZ). A plexus of small vessels surrounding the ventricular system indicated the subventricular zone (SVZ) at the interface between VZ and IZ (Fig. 4). The development of the IZ proceeded caudally and rostrally and reached the cortical anlage at approximately 10 weeks (50 mm CRL). The direction of the processes in IZ was radial, but most sections were cut tangentially to the ventricular surface, resulting in a fragmented pattern (Fig. 3).

From the time when the neural wall exhibited three layers, a receeding of the vimentin-reactivity occurred, so that the outer layers became progressively less stained. The VZ remained vimentin-positive throughout the period studied. The reactivity became located in the cells the furthest away from the ventricular surface, forming a borderline towards the SVZ (Fig. 5). There were only very few vimentin-positive apical processes extending from the positive perinuclear region. As the VZ transformed into ependyma, the ependymal cells remained stained. Cells with the morphology of fibrous astrocytes appeared at about 14 weeks (148 mm CRL) in the midline of the brainstem (Fig. 6).

Mitoses. Adjacent to the ventricular surface frequent vimentin-positive mitotic figures were observed in all regions in the embryos and early fetuses (Figs. 1, 2B, 7).

Endfeet. With only a few exceptions mentioned below, the dense packing of endfeet only lasted until the development of MZ. Where lamination occurred, the vimentin-positive endfeet disappeared gradually, following the pattern seen in the myelencephalon which was the first region to exhibit a change. At early stages the vimentin-positive endfeet exhibited a nearly continuous layer (Fig. 2A, B). Later, vi-

Fig. 3. In the rhombencephalon of a 15 mm CRL embryo, thin vimentin-positive processes are radial (*arrows*) in the intermediate zone (*IZ*) and both tangential (*arrowhead*) and radial in the marginal zone (*MZ*) × 530

Fig. 4. In the rhombencephalon of a 15 mm CRL embryo, the ventricular zone (*VZ*) exhibits vimentin-positive NE cells and thick radial processes. The change of direction of radial processes in the intermediate zone (*IZ*) results in cross-sectioned processes (*arrows*). Small vessels are indicated by *arrowheads*. × 530

Fig. 5. The brain stem of a 62 mm CRL fetus exhibits perinuclear vimentin-immunoreaction in the basal part of the ventricular zone (*VZ*). *IZ*, intermediate zone. *VS*, ventricular surface. × 930

Fig. 6. In the midline of the brainstem of a 148 mm CRL fetus vimentin-positive fibrous astrocytes are indicated by *arrows*. Vessels (*arrowheads*) are incompletely surrounded by vimentin-reactivity. × 630

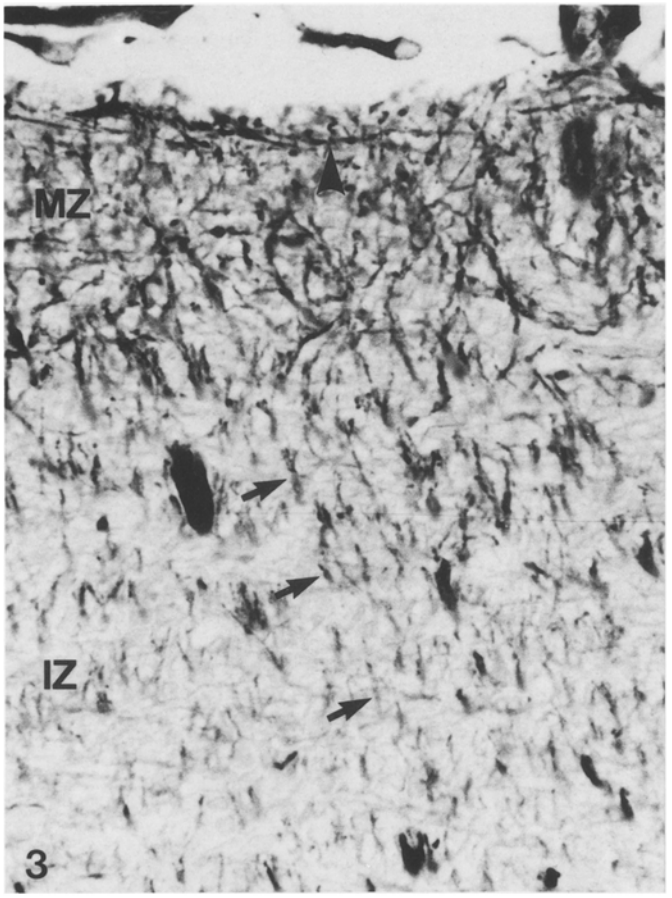

3

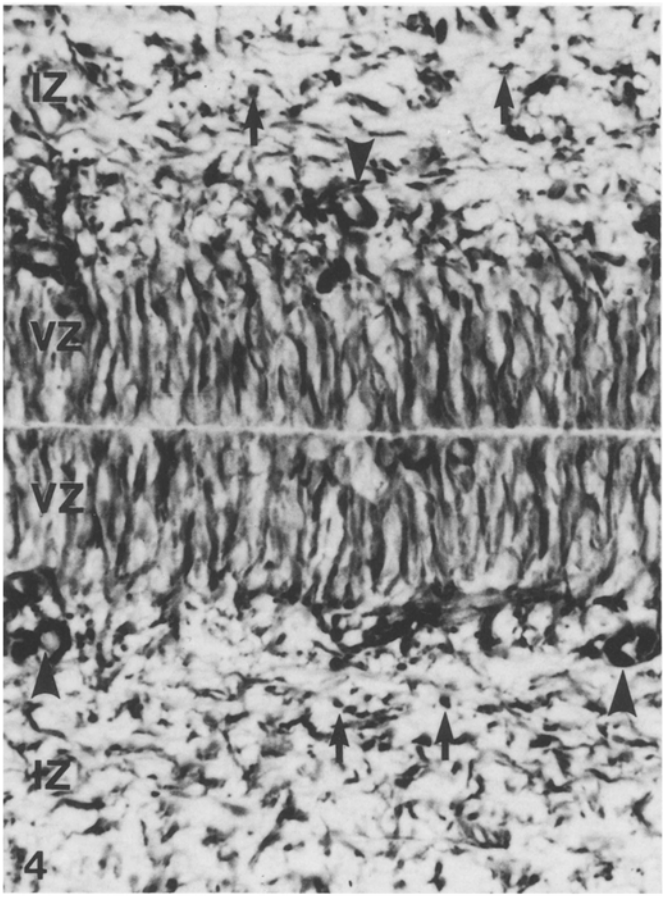

4

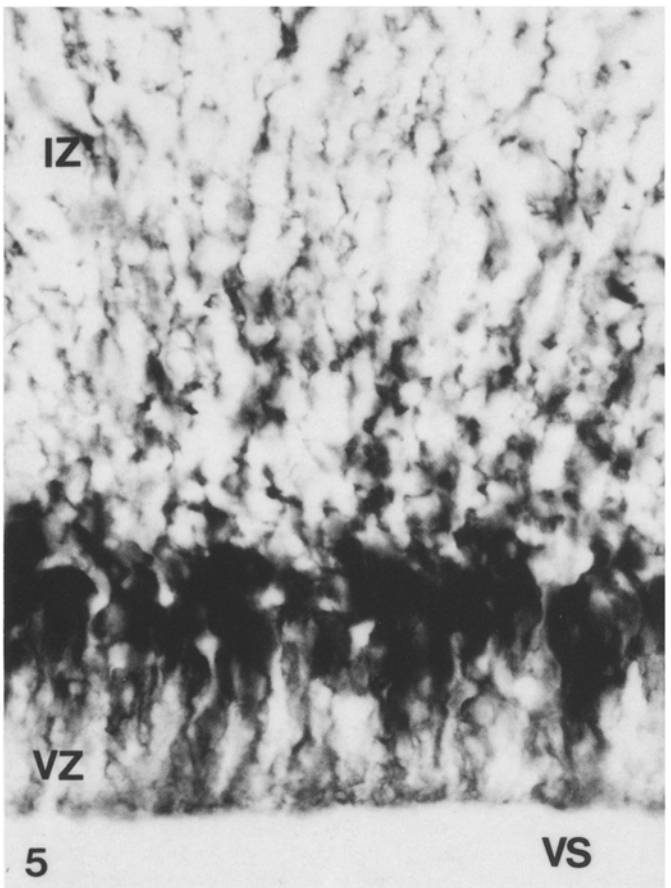

5

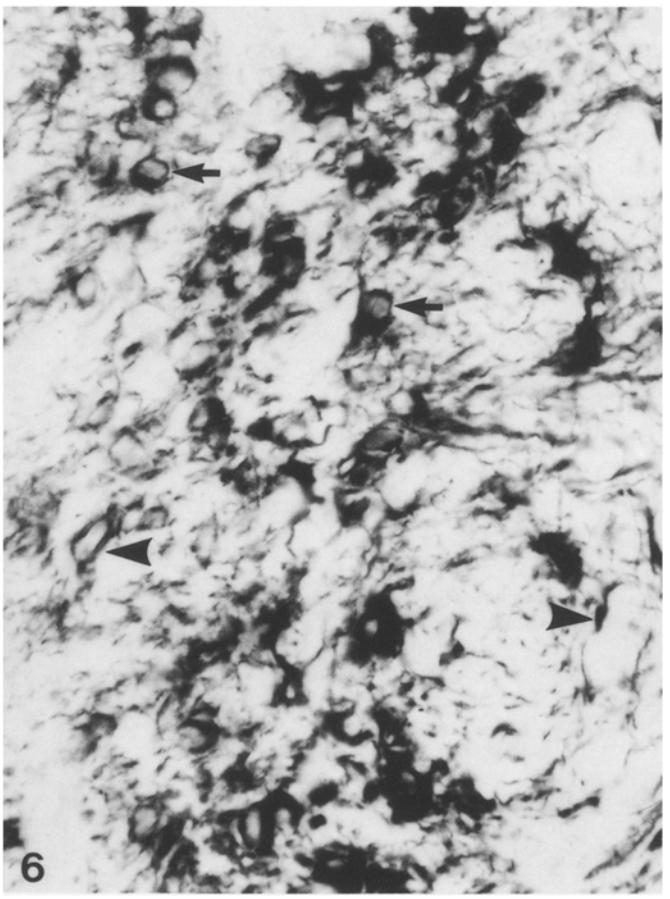

6

mentin-negativity was predominant, but single, intensely stained endfeet were seen scattered at the pial surface (Figs. 3, 10).

Regional differences

In the previous paragraphs we have described an overall developmental pattern of vimentin-reactivity in the neuroepithelium. There are, however, characteristic regional differences concerning the finer morphology of the NE cells. In the *lateral telencephalic wall*, the future neocortex, the lamination was established in a distinct manner. As the MZ developed at 7 weeks the "limiting" glial endfeet became vimentin-negative. The thick processes of the VZ terminated abruptly at the VZ-MZ interface, thus forming a demarcation line defined by the presence of numerous rounded structures which resembled endfeet (Fig. 8). This gave the impression that the endfeet had detached from the external limiting membrane and thus from the presumptive pia-arachnoid. The third layer, described in the previous section, appeared during the 8.–9. week as the cortical plate (CP) developed. Sparse fine straight radial processes coursed through the CP, some continued to the MZ but none ended in immunoreactive endfeet (Fig. 8). The processes remained sparse during the entire period of CP development.

The overall development of vimentin-reactivity in *the diencephalon and the brain stem* did not differ significantly from the general pattern already described. The most prominent structure though, was a ventral *midline raphe* exhibiting vimentin-positive radial processes (Fig. 9A), which were not subject to lamination as were the rest of the CNS. The processes spanned the entire neural wall ending at the external surface in conspicuous endfeet, which were as densely packed as those seen in the VZ stage neural tube (Figs. 1, 9A). These processes formed a dense continuous band and extended throughout the CNS from the lamina terminalis of the early prosencephalon, through the diencephalon, brain stem and the spinal cord. The midline raphe was very marked ventrally, but apart from certain regions e.g. in the subcommissural organ and in the spinal cord, it was barely recognizable dorsally. Also located in the midline were the tanycytes of the median eminence. They were intensely immunostained, and spanned the wall from the bottom of the third ventricle to the external surface, where their endings appeared exceptionally large.

The spinal cord was the only region, which did not develop the characteristic three layers but during the 5.–6. week the spinal cord exhibited two layers with thick processes in VZ and thin ones in MZ. As the IZ developed, the thin radial processes spanned in a divergent manner from the VZ to the external surface, where all processes ended in bulbous endfeet (Fig. 10). At later stages the vimentin-positive radial processes were not in visible contact with the ependyma, but were still present in the IZ and MZ, ending in single prominent endfeet. These radial processes seemingly separated the ascending and descending fibers into fascicles. This was more pronounced in the basal plate anterolaterally than in the alar plate. Radial processes and endfeet remained vimentin-positive throughout the period studied, although in continuously diminishing numbers.

The columnar epithelium of the early developing *choroid plexus* at 7 weeks exhibited vimentin-immunoreactivity in a pattern different from that seen in other parts of the neuroepithelium: At adjacent cell membranes and at the apex of the cells a fine rim of immunoreactivity was seen. In cells cut tangentially to the ventricular surface, the reactivity was located in the periphery of the cells, and was thus seen as open rings (Fig. 11).

Vimentin-reactivity outside the CNS. In the youngest embryo (4.5 mm CRL) the *notochord*, the *somites*, still epithelial in nature, as well as *lens and otic vesicles* and *the retinal pigment epithelium* were intensely stained in a pattern comparable to what was seen in the neural tube: all cells were vimentin-positive and endfeet were densely packed, lining the external surface (Fig. 12A, B). The notochord and its remnants, the nucleus pulposus, remained stained thorughout the period studied. The somites lost their reactivity concomitantly with their differentiation into sclero-, derma-, and myotomes, though the slightly later developing myotubes showed a reactivity, which was later to be replaced by desmin-reactivity. The lens and otic vesicles exhibited immunoreactivity during the embryonic period, after which it was gradually diminishing.

Anti-vimentin antibodies also stained vessels both in- and outside the CNS (Figs. 4, 11). There was no positive staining reaction in epithelia of e.g. gut including the Rathke's pouch, and kidney anlage.

Immunoreactivity to other cellular marker antibodies

In an attempt to elicit similar patterns of reactivity, four different antibodies to *vimentin* were applied. The clone V9 (Dakopatts, DK) was by far the one giving the best results, with distinctly outlined immunoprecipitates and no background staining. This antibody was used for all illustrations. An identical staining pattern was obtained by the antibody from Labsystems, but in our hands with unacceptable background staining. Although the two antibodies

Fig. 7. In the telencephalic ganglionic eminence of a 24 mm CRL embryo vimentin-positive mitoses (*arrowheads*) are frequent in the ventricular zone (*VZ*). *VS*, ventricular surface. × 580

Fig. 8. The lateral telencephalic wall of a 20 mm CRL embryo exhibits endfeet-resembling structures (*arrows*) at the interface between ventricular (*VZ*) and intermediate zones (*IZ*). The long arrow indicates the transition from the middle (*IZ*) to the outer third (*MZ*) layer of the vimentin-immunoreactivity pattern. There are no vimentin-positive endfeet at the external surface, but vessels outside the CNS are stained (*arrowhead*). × 430

Fig. 9. A The midline raphe (*R*) in the brainstem of a 62 mm CRL fetus is intensely vimentin-positive. Radial processes (*arrows*) span from the ventricular surface (*VS*) towards the pia-arachnoid (*PA*), in a pattern which is quite similar to that of GFA-reactivity (**B**). × 95. **B** Neighbouring section to **A**, stained with Dakopatts' anti-GFA antiserum. The midline raphe (*R*) is GFA-negative except for some fibrous astrocytes (*open arrows*). There is a slight accumulation of radial processes adjacent to the raphe (*arrowheads*). *Arrows*, radial processes; *VS*, ventricular surface; *PA*, pia-arachnoid. × 95

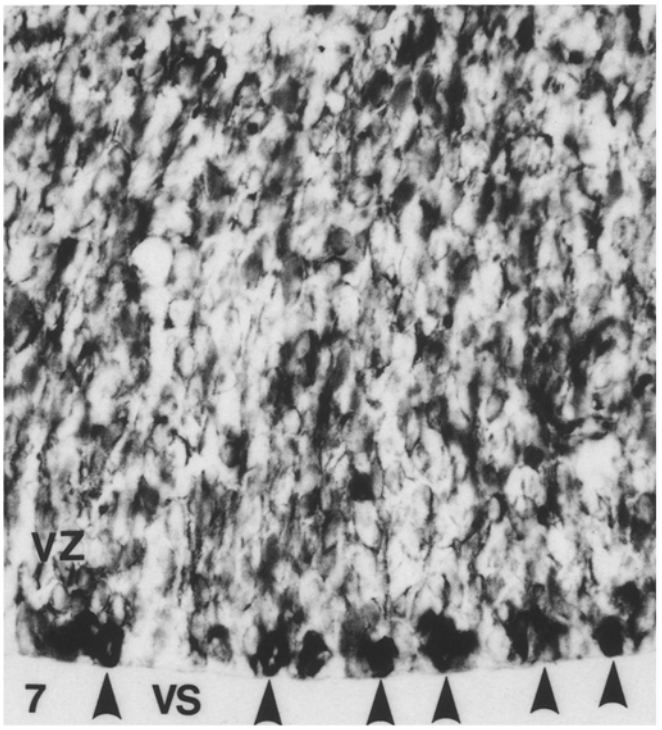
VZ
7
VS

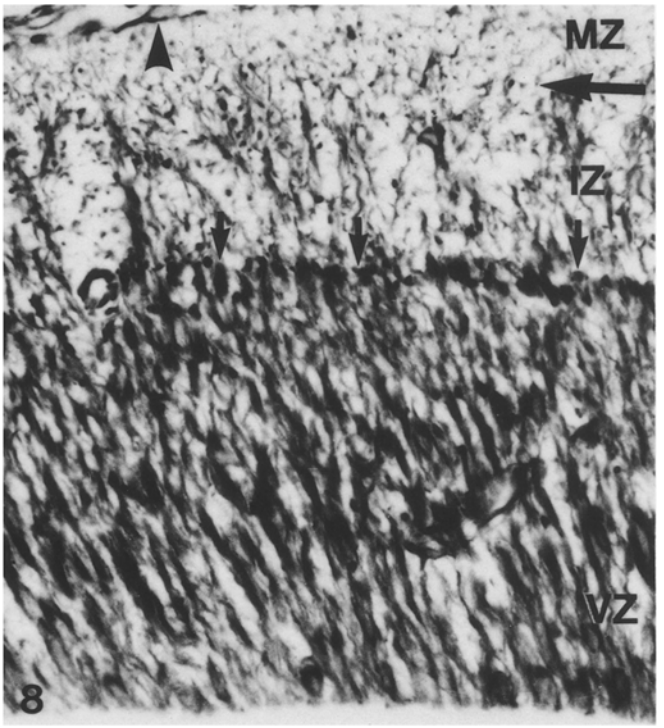
MZ
IZ
VZ
8

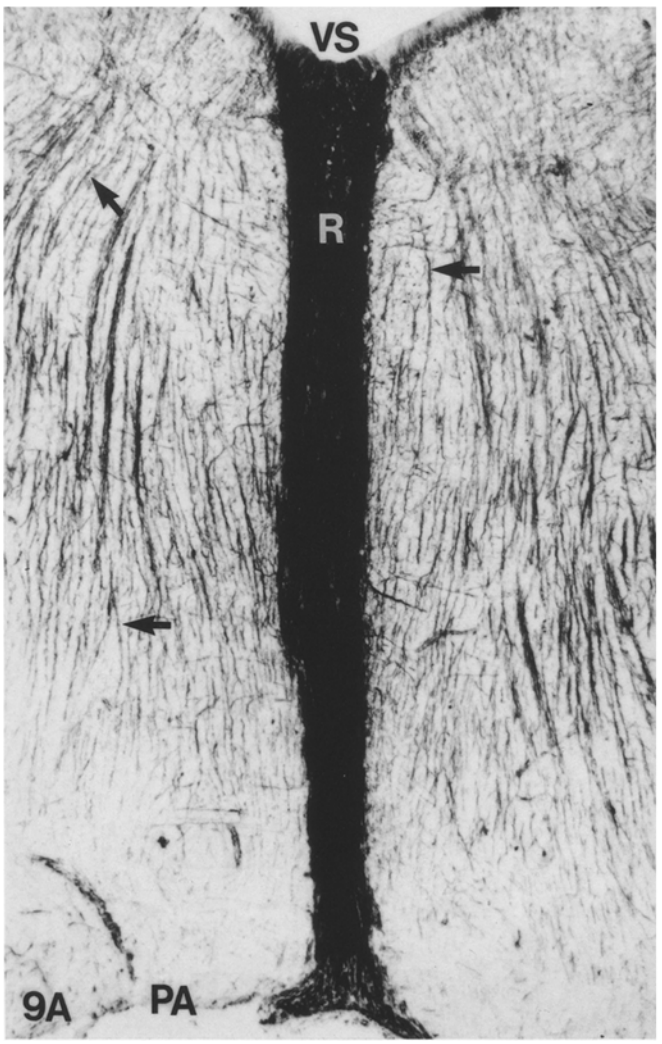
VS
R
9A
PA

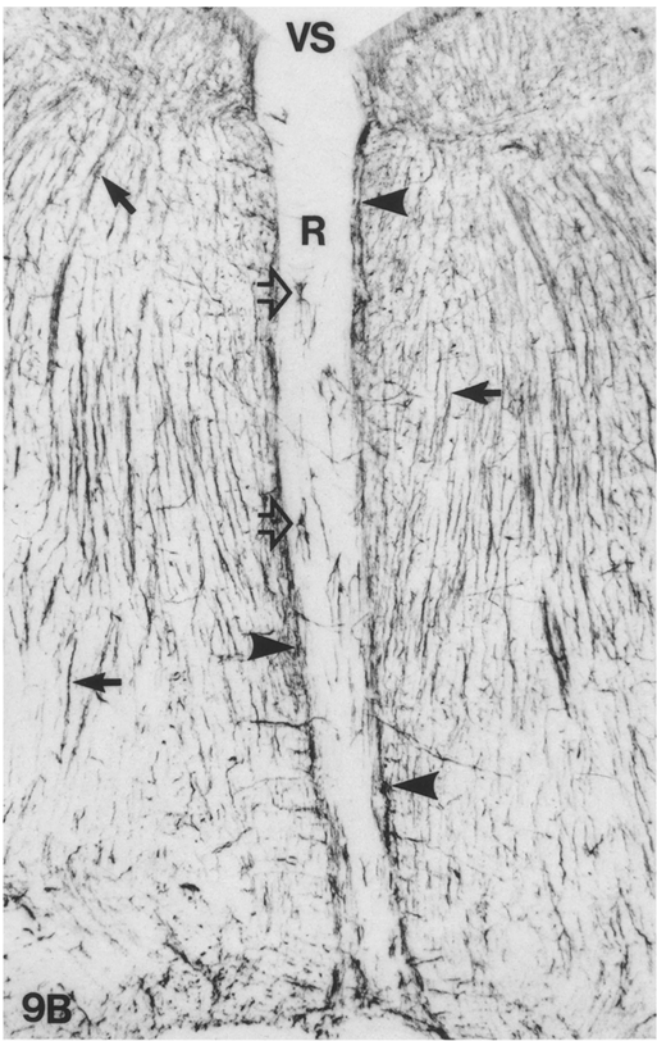
VS
R
9B

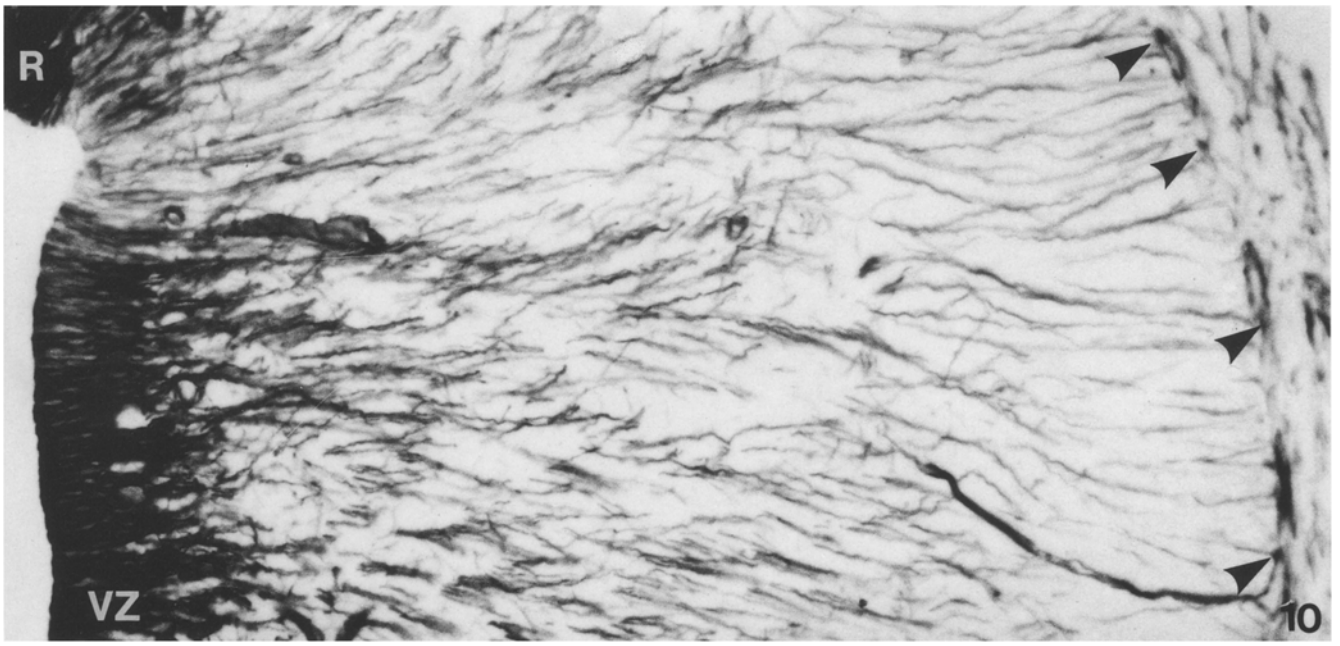
R
VZ
10

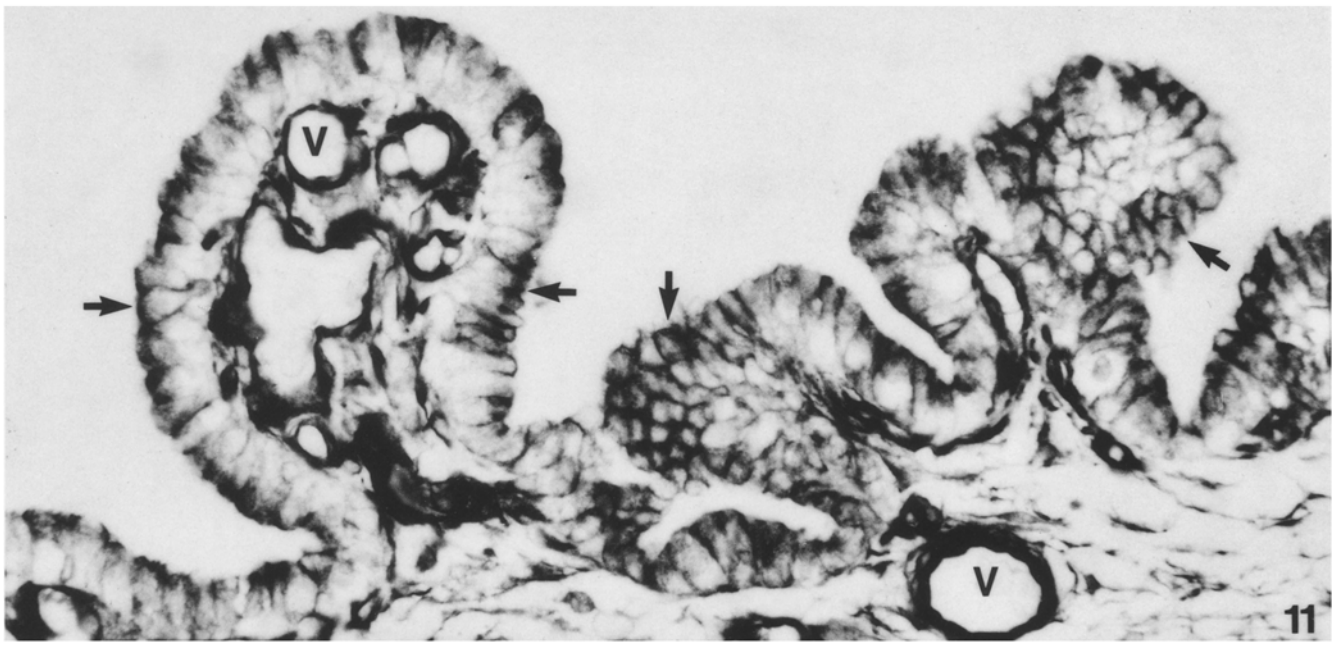
V
V
11

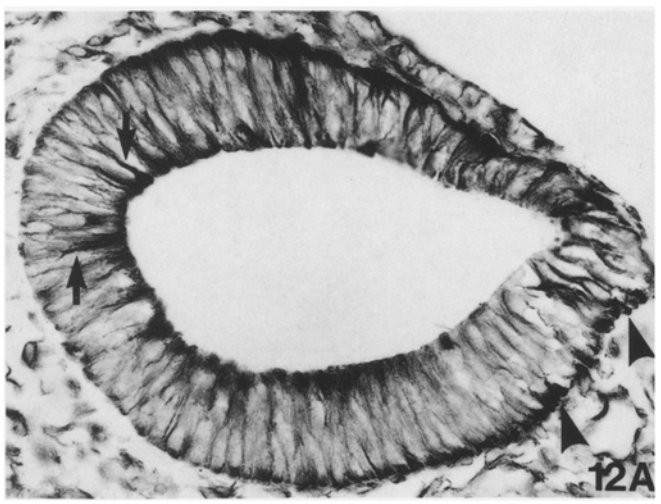
12A

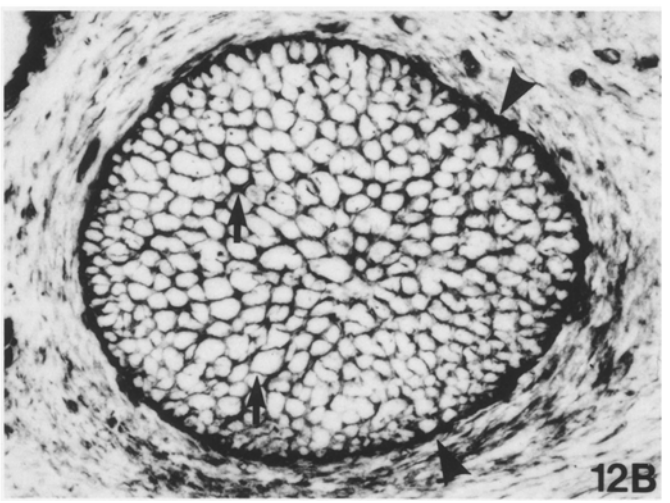
12B

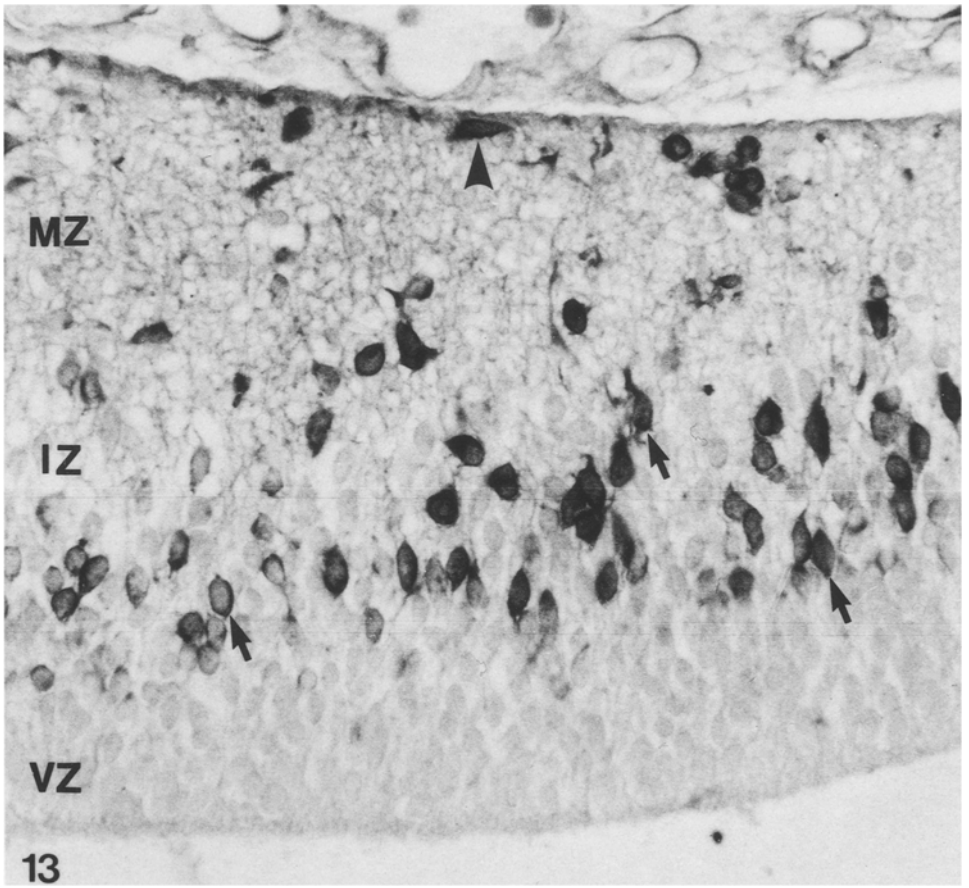

Fig. 13. Cells in the medial telencephalic wall in a 20 mm CRL embryo, resembling young migrating neurons (*arrows*) in the presumptive intermediate zone (*IZ*), are desmin-immunoreactive. In the marginal zone (*MZ*) a Cajal-Retzius cell is also desmin-positive (*arrowhead*). *VZ*, ventricular zone. × 520

from Sigma had weak reactions, all four antibodies had similar reaction patterns (see Osborn et al. 1984).

One of the four monoclonal anti-*cytokeratin* antibodies (from Becton-Dickinson: CAM 5.2) immunostained restricted areas in the CNS: The choroid plexus in the lateral, third and fourth ventricles and the transition zones between the choroid plexus and the VZ were cytokeratin-positive, exhibiting a pattern similar to that of vimentin-immunoreaction, although cytokeratin was only detected in a small percentage of the vimentin-positive cell population. Remnants of the notochord, which regresses into the nucleus pulposus, were intensely stained and the cells of the otic vesicle were immunostained as described in the paragraph on vimentin. The meninges were cytokeratin-positive following staining with the CAM 5.2 monoclonal antibody as well as with the polyclonal antibody, both of which reacted with the peritoneum, pleura and epithelia in intestines, kidney, and pancreas, and in the case of the polyclonal antibody, with epidermis.

A distinct reaction to anti-*desmin* antiserum was found in the telencephalic walls at stages when the CP was developing. In the medial telencephalic wall bipolar radially orientated presumptive young neurons were scattered in the IZ, and single horizontal perikarya in the MZ were desmin-positive (Fig. 13). Morphologically similar cells were stained in the MZ of caudal-most part of the rhombic lip. In the lateral wall desmin-immunoreaction was seen only in tangential fibers immediately above and below the CP. Both the lateral and the medial telencephalic walls were desmin-negative in the VZ, and the latter exhibited no reaction in tangential fibers. Outside the CNS only myotubes and developing muscles were desmin-positive.

When reactivity to anti-*GFA* antibodies appeared, the pattern resembled that of vimentin at the same stage, and

Fig. 10. In the spinal cord of a 20 mm CRL embryo the ventricular zone (*VZ*) and anterior midline raphe (*R*) are intensely vimentin-positive. The weak immunostaining just lateral to the midline raphe was a constant finding. Radial processes extend to the external surface, ending in single endfeet (*arrowheads*). × 250

Fig. 11. Choroid plexus of the fourth ventricle in a 28 mm CRL embryo. The vimentin-immunoreaction is restricted to the periphery of the apical part of the plexus cells (*arrows*). Vessels (*V*) in the plexus stroma are also stained. × 500

Fig. 12. **A** The otic vesicle in a 4.5 mm CRL embryo exhibits vimentin-positive cells (*arrows*) which possess endfeet at the ventricular surface (*arrowheads*). × 380. **B** The otic vesicle in a 38 mm CRL embryo is tangentially cut and exhibits perinuclear vimentin-immunostaining (*arrows*) and a continuous layer of vimentin-immunostaining (*arrows*) and a continuous layer of vimentin-positive endfeet (*arrowheads*). × 200

in all regions cells in the basal VZ were stained. In the brain stem and spinal cord radial processes were GFA-positive and reactivity developed in single endfeet throughout the CNS. There was an accumulation of immunoreactive radial processes in the dorsal midline of the spinal cord, whereas the ventral GFA-negative midline raphe was outlined by radial processes which spanned from the ventricular to the external surfaces, lateral to the raphe (Fig. 9B).

Reactivity to anti-*S-100* antiserum developed relatively early (8 weeks) in the spinal cord, where ventricular cells, radial processes and their endfeet were stained. The ventral midline raphe was not stained. Astrocytes were stained with both anti-GFA and anti-S-100 antibodies at considerably earlier stages than seen with anti-vimentin antibodies.

Anti-*NF* and anti-*NSE* antibodies labeled longitudinal and horizontal fibers in MZ in the brain stem in 7-week-old embryos. The development of NF immunostaining followed a ventral to dorsal gradient in addition to the developmental gradient already described with a starting point in the lower rhombencephalon. No staining was seen in the VZ.

Discussion

Vimentin was originally isolated from and described in cultured fibroblasts (Franke et al. 1978), and was later detected in the neuroepithelium of vertebrates (Schnitzer et al. 1981; Tapscott et al. 1981; Bignami et al. 1982). Vimentin has been reported to appear in the mouse neuroepithelium on embryonic day 9 (E9), a stage when the first half of the somites has developed (Houle and Fedoroff 1983), although a slight variation from species to species has been observed (Tapscott et al. 1981; Bignami et al. 1982; Erickson et al. 1987). The youngest embryo of our collection represents a stage, when most of the somites have developed (4 weeks), thus the vimentin-immunoreactivity of all human neuroepithelial cells corresponds well with reported findings in other species. Sasaki et al. (1988) studied the early human fetal CNS and demonstrated vimentin in columnar cells in the neural tube, and in ventricular cells in the spinal cord and cerebrum. This is in accordance with our results, although the same commercially available antibody elicited an immunoreaction in our material, which was much more extensive and stained all cells in the neural tube, including mitotic figures. Our findings of slender radial processes in both IZ and MZ in the neural wall are not previously reported.

The accumulation of radial processes in the midline of the brainstem and spinal cord is well known (see van Hartesveldt et al. 1986). In our material, the *ventral midline raphe* was extensively immunostained by anti-vimentin antibodies, revealing a thick bundle of radial processes, which terminated in prominent endfeet at the external ventral surface. Vimentin or vimentin-like reactivity has also been illustrated in the ventral midline raphe of chicken (Tapscott et al. 1981) and rat (Hockfield and McKay 1935). The raphe proper was S-100-negative as well as GFA-negative, whereas GFA-positive radial processes lateral to the ventral midline raphe and in radial processes in the dorsal midline have been demonstrated in several species: human (Lauriola et al. 1987; Sasaki et al. 1988; the present study), monkey (Levitt and Rakic 1980, Figs. 17A, B), rat (van Hartesveldt et al. 1986) and chicken (Tapscott et al. 1981). The possible function of the raphe will be discussed later.

The vimentin-positive cell population in human embryonic and fetal brain was compared with and distinguished from other cell populations by the application of a range of antibodies. This enabled us to exclude the possibility of cross-reactivity of the anti-vimentin antibodies because the immunoreactivity patterns of the other intermediate filaments only partly overlapped.

The *cytokeratin*-immunoreaction (No. 8, 18, 19) included the notochord and the otic vesicle but not the neural tube or neural wall. These findings are in accordance with what is seen in the rabbit embryo (Viebahn et al. 1988), whereas the presence of mixed cytokeratins in central ependymal septa in adult *Xenopus laevis* spinal cord (Szaro and Gainer 1988), does not seem to have a counterpart in rabbit (Viebahn et al. 1987), quail (Erickson et al. 1987), or human spinal cord. The perinuclear, ring-like distribution of vimentin and of cytokeratin in the choroid plexus cells, which is seen also in adult plexus (Kasper et al. 1986, Fig. 3), corresponds to the localization of intermediate filaments in contact with zonulae adherentes described by Hudspeth and Yee (1973) in retinal pigment epithelium. For discussion of the functional significance of cytokeratin and its coexpression with vimentin see Erickson et al. 1987 and Kasper et al. 1988.

A surprising finding was the presence of *desmin*-immunoreactive single cells in the embryonic telencephalon. The nature of the desmin-positive cells is uncertain, but based on morphology, time of appearance, and location they resemble young migrating neurons and Cajal-Retzius cells. Desmin has not been reported to be present in neurons, but Dahl et al. (1986) has demonstrated desmin-immunoreactivity in astrocytes.

GFA was the only intermediate filament which had an immunoreaction pattern similar although not identical to that of vimentin. The patterns of GFA and vimentin reactivities in the VZ strongly suggest a colocalization, but further evidence of a colocalization in these densely packed and very narrow cells will require electronmicroscopic detection. In other species GFA has been reported to be transiently colocalized with vimentin in cells of the VZ and in radial processes (Dahl et al. 1981; Bovolenta et al. 1984; Sasaki et al. 1988). GFA-positive mitotic figures in VZ cells were seen in monkey fetal brain (Levitt et al. 1983), but have not been reported in human material by previous investigators (e.g. Roessmann and Gambetti 1986; Reske-Nielsen et al. 1987; Sasaki et al. 1988).

NF and NSE were distributed in characteristic and almost identical patterns, corresponding to those seen previously in human fetal brain (Windle 1970; Shinohara et al. 1986; Sasaki et al. 1988); the patterns were distinctly different from those of vimentin and GFA. In other species NF has been found to be colocalized transiently with vimentin in NE cells (rat: Dahl et al. 1981; Bignami et al. 1982) including mitotic NE cells (mouse: Cochard and Paulin 1984; chicken: Bennett and DiLullo 1985). No NF reactivity was found in mitotic figures of VZ cells in our fetal material.

The vimentin-positive radial processes, which developed as the neural wall became laminated, were morphologically quite similar to the processes of radial glial cells, which are seen following Golgi staining or GFA-immunocytochemistry (see e.g. Rakic 1981a; Choi 1981; Levitt and Rakic 1980). Radial glial cells act as guides for the migrating young neurons (Rakic 1971, 1981a; Hatten et al. 1984), so the function of the radial glial cells and thus of vimentin

is probably not coupled to the motility of the vimentin-positive cells themselves. Rather, the vimentin-positive cells may mediate and modulate the migration of neighbouring cells, which might be a prerequisite for correct tempero-spatial migration and establishment of radial columns (Rakic 1981 b).

The function of the midline raphe is unknown, but its transient presence, which is equivalent to the existence of radial glial cells, and its lack of "mature" glial markers could suggest that this structure in some way also mediates or modulates the migration of other cells (Szaro and Gainer 1988). It could for example act as a "freeway", on which cells could migrate and axons could grow. At the same time, by forming a boundary between the two halves of the brain (van Hartesveldt et al. 1986), it could prevent "premature" crossing over and formation of connections across the midline, which might occur only when the raphe has disappeared or has become vimentin-negative. In analogy, tangential growth of e.g. the first incoming fibers from the brain stem to the MZ (Lidov and Molliver 1982) would only be "allowed" to occur when the neural wall exhibits lamination due to vimentin-negativity of the radial glial processes in the MZ.

Vimentin is not present in very early stages of mouse neural tube development, but appears in embryos at E9 (15–20 somites), and increases significantly from E9 to E10 (30–34 somites) according to Houle and Fedoroff (1983). In a number of other species vimentin has been detected in the neuroepithelium at comparable stages (see Introduction for Refs.). The youngest of our embryos, the stage of which would correspond to E10 in the mouse, also exhibited intense vimentin-immunoreactivity in all NE cells. It seems that all NE cells start out as vimentin-negative, go through a stage of vimentin-positivity, and then gradually stop their vimentin expression. Whether vimentin is a general marker for cell maturity and cell differentiation (Houle and Fedoroff 1983), can be questioned after results obtained with cell cultures from mouse neural plate (Buse 1987). When vimentin-negative NE cells from $E7^1/_2$ mouse were cultured, they did not express vimentin, but reproducibly transformed into cell groups, which expressed various neuronal marker molecules. It remains unsettled whether some cell groups are actually determined at this early stage in the neural plate, but the culture conditions might have induced determination and differentiation of specific cells types (Raff et al. 1983), in some way bypassing and making the vimentin-positive stage unnecessary.

The function of vimentin has been suggested to relate to cell motility e.g. in embryonic neural crest cells (cf. Erickson et al. 1987; Viebahn et al. 1988). The vimentin-positive cells of the neural tube do not migrate themselves, since they are attached to one another by junctional complexes at the ventricular surface (Hinds and Ruffet 1971; Møllgård et al. 1987), but the nuclei of these cells exhibit interkinetic to-and-fro movements, where nuclei move from apical to basal positions in the neural wall during mitotic cycles (Sauer 1936). At later stages as the CNS becomes laminated and increases in depth, it seems likely that the interkinetic movements would be limited to the VZ, which continues to be vimentin-positive; thus the nuclear migration would not involve the entire neural wall. It remains to be elucidated whether vimentin has any functional relationship with the interkinetic nuclear migration in the VZ. If this is so, it might explain the lack of vimentin-expression in the cultured NE cells (Buse 1987), as the cells were dissociated and cultured in monolayer without the possibility to develop into the normal pseudostratified epithelium. The bypassing of a vimentin-positive stage may be explained by morphological as well as biochemical constraints or alterations. The nature of the vimentin-positive NE cells is thus an open question. They can be perceived as an apparently homogeneous cell population differentiated to the point, where vimentin is expressed, and from where the cells can develop other specialized functions.

Acknowledgements. We wish to thank Keld Bo Ottesen for excellent technical assistance. The study was supported by Warwara Larsens Fond.

References

Alvarez-Buylla A, Buskirk DR, Nottebohm F (1987) Monoclonal antibody reveals radial glia in adult avian brain. J Comp Neurol 264:159–170

Antanitus DS, Choi BH, Lapham LW (1976) The demonstration of glial fibrillary acidic protein in the cerebrum of the human fetus by indirect immunofluorescence. Brain Res 103:613–616

Bennett GS, Lullo S (1985) Transient expression of a neurofilament protein by replicating neuroepithelial cells of the embryonic chick brain. Dev Biol 107:107–127

Bignami A, Raju T, Dahl D (1982) Localization of vimentin, the nonspecific intermediate filament protein in embryonal glia and in early differentiating neurons. Dev Biol 91:286–295

Bovolenta P, Liem RKH, Mason CA (1984) Development of cerebellar astroglia: Transition in form and cytoskeletal content. Dev Biol 102:248–259

Boulder Comittee (1970) Embryonic vertebrate central nervous system: revised terminology. Anat Rec 166:257–261

Buse E (1987) Ventricular cells from the mouse neural plate, Stage Theiler 12, transform into different neuronal cell classes in vitro. Anat Embryol 176:295–302

Choi BH (1981) Radial glia of developing human fetal spinal cord: Golgi, immunohistochemical and electron microscopic study. Dev Brain Res 1:249–267

Choi BH, Lapham LW (1978) Radial glia in the human fetal cerebrum: A combined Golgi, immunofluorescent and electron microscopic study. Brain Res 148:295–311

Choi BH, Lapham LW (1980) Evolution of Bergmann glia in developing human fetal cerebellum: A Golgi, electron microscopic and immunofluorescent study. Brain Res 190:369–383

Cochard P, Paulin D (1984) Initial expression of neurofilaments and vimentin in the central and peripheral nervous system of the mouse embryo in vivo. J Neurosci 4:2080–2094

Dahl D (1981) The vimentin-GFA transition in rat neuroglia cytoskeleton occurs at the time of myelination. J Neurosci Res 6:741–748

Dahl D, Ruegger DC, Bignami A, Weber K, Osborn M (1981) Vimentin, the 57000 dalton protein of fibroblast filament, is the major cytoskeletal component in immature glia. Eur J Cell Biol 24:191–196

Dahl D, Zapatka S, Bignami A (1986) Heterogeneity of desmin, the muscle-type intermediate filament protein, in blood vessels and astrocytes. Histochem 84:145–150

Erickson CA, Tucker RP, Edwards BF (1987) Changes in the distribution of intermediate filament types in Japanese quail embryos during morphogenesis. Differentiation 34:88–97

Franke WW, Schmid E, Osborn M, Weber K (1978) Different intermediate-sized filaments distinguished by immunofluorescence microscopy. Proc Natl Acad Sci USA 75(10):5034–5038

Hansen SH, Stagaard M, Møllgård K (1989) Neurofilament-like pattern of reactivity in human foetal *PNS* and spinal cord following immunostaining with polyclonal anti-glial fibrillary acidic protein antibodies. J Neurocytol 18: (In press)

Hatten ME, Liem RKH, Mason CA (1984) Two forms of cerebellar glial cells interact differently with neurons in vitro. J Cell Biol 98:193–204

Hinds JW, Ruffet TL (1971) Cell proliferation in the neural tube: an electron microscopic and Golgi analysis in the mouse cerebral vesicle. Z Zellforsch 115:226–264

His W (1889) Die Neuroblasten und deren Entstehung im embryonal Marke. Abh Math Phys Cl Kgl Sach Ges Wiss 15:313–372

Hockfield S, McKay RDG (1985) Identification of major cell classes in the developing mammalian nervous system. J Neurosci 5:3310–3328

Houle J, Fedoroff S (1983) Temporal relationship between the appearance of vimentin and neural tube development. Dev Brain Res 9:189–195

Hudspeth AJ, Yee AG (1973) The intercellular junctional complexes of retinal pigment epithelia. Invest Ophthalmol 12:354–365

Kasper M, Goertchen R, Stosiek P, Perry G, Karsten U (1986) Coexistence of cytokeratin, vimentin and neurofilament protein in human choroid plexus. An immunohistochemical study of intermediate filaments in neuroepithelial tissues. Virchows Arch [A] 410:173–177

Kasper M, Moll R, Stosiek P, Karsten U (1988) Patterns of cytokeratin and vimentin expression in the human eye. Histochem 89:369–377

Lauriola L, Coli A, Cocchia D, Tallini G, Michetti F (1987) Comparative study by S-100 and GFAP immunohistochemistry of glial cell populations in the early stages of human spinal cord development. Dev Brain Res 37:251–255

Levitt P, Rakic P (1980) Immunoperoxidase localization of glial fibrillary acidic protein in radial glial cells and astrocytes of the developing Rhesus monkey brain. J Comp Neurol 193:815–840

Levitt P, Cooper ML, Rakic P (1983) Early divergence and changing proportions of neuronal and glial precursor cells in the primate cerebral ventricular zone. Dev Biol 96:472–484

Lidov HGW, Molliver ME (1982) An immunohistochemical study of seretonin neuron development in the rat: Ascending pathways and terminal fields. Brain Res Bull 8:389–430

Marin-Padilla M (1983) Structural organization of the human cerebral cortex prior to appearance of the cortical plate. Anat Embryol 168:21–40

Møllgård K, Jacobsen M (1984) Immunohistochemical identification of some plasma proteins in human embryonic and fetal forebrain with particular reference to the development of the neocortex. Dev Brain Res 13:49–63

Møllgård K, Balslev Y, Lauritzen B, Saunders NR (1987) Cell junctions and membrane specializations in the ventricular zone (germinal matrix) of the developing sheep brain: a CSF-brain barrier. J Neurocytol 16:433–444

Osborn M, Debus E, Weber K (1984) Monoclonal antibodies specific for vimentin. Eur J Cell Biol 34:137–143

Raff MC, Miller RH, Noble M (1983) A glial progenitor cell that develops in vitro into an astrocyte or an oligodendrocyte depending on culture medium. Nature 303:390–396

Rakic P (1971) Guidance of neurons migrating to the fetal monkey neocortex. Brain Res 33:471–476

Rakic P (1981a) Developmental events leading to laminar and areal organization of the neocortex. In: Schmitt FO (ed) The organization of the cerebral neocortex. MIT Press, Cambridge Massachusetts London, pp 6–16

Rakic P (1981b) Neuronal-glial interaction during brain development. Tr Neurosci 7:184–187

Rickmann M, Amaral DG, Cowan WM (1987) Organization of radial glial cells during the development of the rat dentate gyrus. J Comp Neurol 264:449–479

Reske-Nielsen E, Oster S, Reintoft I (1987) Astrocytes in the prenatal central nervous system. Acta Pathol Microbiol Immunol Scand Sect A 95:339–346

Roessmann U, Gambetti P (1986) Astrocytes in the developing human brain. An immunohistochemical study. Acta Neuropathol 70:308–313

Sasaki A, Hirato J, Nakazato Y, Ishda Y (1988) Immunohistochemical study of the early human fetal brain. Acta Neuropathol 72:128–134

Sauer FC (1936) The interkinetic migration of embryonic epithelial nuclei. J Morphol 60:1–11

Schnitzer J, Franke WW, Schachner M (1981) Immunocytochemical demonstration of vimentin in astrocytes and ependymal cells of developing and adult mouse nervous system. J Cell Biol 90:435–447

Shinohara H, Semba R, Kato K, Kashiwamata S, Tanaka O (1986) Immunohistochemical localization of gamma-enolase in early human embryos. Brain Res 282:33–38

Szaro BG, Gainer H (1988) Immunocytochemical identification of non-neuronal intermediate filament proteins in the developing *Xenopus laevis* nervous system. Dev Brain Res 43:207–224

Tapscott SJ, Bennett GS, Toyama Y, Kleinbart F, Holtzer H (1981) Intermediate filament proteins in the developing chick spinal cord. Dev Biol 86:40–54

van Hartesveldt C, Moore B, Hartman BK (1986) Transient midline raphe glial structure in developing rat. J Comp Neurol 153:175–184

Varon SS, Somjen GG (1979) Neuron-glia interactions. Neurosciences Res Prog Bull, vol 17, No 1

Viebahn C, Lane EB, Ramaekers FCS (1988) Keratin and vimentin expression in early organogenesis of the rabbit embryo. Cell Tissue Res 253:553–562

Windle WF (1970) Development of neural elements in human embryos of four to seven weeks gestation. Exp Neurol [Suppl] 5:44–70

Accepted January 5, 1989